Published paper
Yang, H., Gibson, S. and Tomlinson, R.A. (2006) *Improvement of Fourier Polarimetry for applications in tomographic photoelasticity.* Experimental Mechanics, 46 (5). pp. 619-626.
http://dx.doi.org/10.1007/s11340-006-9112-7

Improvement of Fourier Polarimetry for Applications in Tomographic Photoelasticity

H. Yang, S. Gibson and R. A. Tomlinson

Department of Mechanical Engineering, the University of Sheffield
Mappin Street, Sheffield, S1 3JD, UK
Email r.a.tomlinson@sheffield.ac.uk

Abstract

The use of the Fourier Polarimetry method has been demonstrated to extract the three characteristic parameters in integrated photoelasticity. In contrast to the phase-stepping method, it has been shown that the Fourier method is more accurate. However, the Fourier method isn't very efficient as it requires that a minimum of nine intensity images be collected during a whole revolution of a polarizer while the phase-stepping method only needs six intensity images.

In this paper the Fourier transformation is used to derive the expression for determination of the characteristic parameters. Four Fourier coefficients are clearly identified to calculate the three characteristic parameters. It is found that the angular rotation ratio could be set arbitrarily. The angular rotation ratio is optimized to satisfy the requirements of efficiency and proper data accuracy, which results in data collection about 3 times faster than the methods suggested by previous researchers. When comparing their performance in terms of efficiency and accuracy, the simulated and experimental results show that these angular rotation ratios have the same accuracy but the optimized angular rotation ratio is significantly faster.

The sensitivity to noise is also investigated and further improvement of accuracy is suggested.

1. Introduction

It is well known that tomography is a powerful tool for the determination of the internal structure of a 3D object; however, the technique is only available for scalar fields. The problem of recovering the full stress tensor field from photoelastic measurements has been addressed mathematically recently. Tomographic photoelasticity proposed by Hammer et al. [1] allows the non-destructive determination of the 3-D stress distributions in weak-birefringent materials. The method employs a two-dimensional Radon inverse transformation to reconstruct one component of the dielectric tensor in the direction of the tomographic rotation axis. The careful selection of the five rotation axes will provide altogether five elements of the anisotropic part of the dielectric tensor. Once the anisotropic dielectric tensor is reconstructed, the deviatoric stress tensor can then be obtained from the stress-optic law and if required the hydrostatic stress recovered from the equilibrium condition.

In order to use a two-dimensional Radon inverse transformation to reconstruct the element of the dielectric tensor, the three characteristic parameters of the 3D object need to be measured at different scanning angles to calculate the unitary transfer matrices [2]. The amount of data to be collected is proportional to the number of scans, which is determined by the required resolution of the reconstructed tensor. At least 36 scans (5 degrees interval) are suggested for tomographic photoelasticity by Szotten et al. [3]. This data needs to be collected as fast as possible and also be of high accuracy. For automatic full-field characteristic parameter measurement, several polarimetric techniques have been developed based on phase-stepping or Fourier analysis. The Fourier analysis-based approach was firstly presented by Berezhna

[4]. The operation of the method consists of synchronous rotation of a polarizer and an analyzer over 360 degrees and the collection of a specified number of subsequent images. Since many images can be combined for Fourier analysis, this reduces the noise and increases the accuracy. In contrast to the phase-stepping method, it has been shown that the Fourier method gives greater accuracy [5]. However, the technique isn't very efficient as it requires that a minimum of nine intensity images be collected during a whole revolution of a polarizer while the phase-stepping method only needs six intensity images [6]. In practise many more images are recorded in the Fourier Polarimetry method to acheive greater accuracy and a larger signal to noise ratio. If the technique is to be used for tomographic photoelasticity, the efficiency needs to be improved.

In the following section the theory of the Fourier method is re-examined to improve the efficiency. The resulting method is verified through both a Matlab simulation and by experiment.

2. Theory

For evaluating the full-field characteristic parameters by the Fourier method, a plane polariscope (shown in Figure 1) is used, with the obvious advantages of its optical arrangement without quarter-wave plates [7]. The principal states of the optical effect introduced by a 3D stressed model on incident light is described as a simple system consisting of a linear retarder, which is represented by the characteristic retardation (denoted by 2Δ) and the primary characteristic direction (denoted by θ), and a rotator, which is represented by the characteristic angle (denoted by γ) [8]. The components of the light vector along the analyzer axis E_{β}, and perpendicular to the analyzer axis $E_{\beta+\pi/2}$, are obtained by Jones calculus as follows:

$$\begin{pmatrix} E_{\beta} \\ E_{\beta+\pi/2} \end{pmatrix} = \begin{pmatrix} \cos\beta & \sin\beta \\ -\sin\beta & \cos\beta \end{pmatrix} \times \begin{pmatrix} \cos\Delta\cos\gamma - i\sin\Delta\cos(2\theta+\gamma) & -\cos\Delta\sin\gamma - i\sin\Delta\sin(2\theta+\gamma) \\ \cos\Delta\sin\gamma - i\sin\Delta\sin(2\theta+\gamma) & \cos\Delta\cos\gamma + i\sin\Delta\cos(2\theta+\gamma) \end{pmatrix} \times \begin{pmatrix} \cos\alpha \\ \sin\alpha \end{pmatrix} ke^{i\omega_t t} \tag{1}$$

where α and β is the angular positions of the polarizer and the analyzer respectively and $ke^{i\omega t}$ is the incident light vector. The experimental data are required at a specific number of the angular positions of the polarizer and the analyzer. For each position the polarizer and the analyzer are set at particular orientations such that $\beta = n\alpha$, where n is an angular rotation ratio of the analyzer to the polarizer. The intensity of light at the output of the polariscope I_{out} can be expressed as

$$I_{out} = I_b + \frac{I_{in}}{2}\begin{bmatrix} 1 + \cos^2\Delta\cos 2\gamma\cos 2(n-1)\alpha \\ +\cos^2\Delta\sin 2\gamma\sin 2(n-1)\alpha \\ +\sin^2\Delta\cos(4\theta+2\gamma)\cos 2(n+1)\alpha \\ +\sin^2\Delta\sin(4\theta+2\gamma)\sin 2(n+1)\alpha \end{bmatrix} \tag{2}$$

where I_{in} is the intensity of the incident light and a constant of proportionality and I_b is intensity of the background and stray light. The output periodic intensity I_{out} can be regarded as the Fourier series in which the Fourier coefficients are functions of the three unknown characteristic parameters. In this way, the three characteristic parameters could be identified by the magnitudes of the spectrum at the angular frequencies of 2(*n*-1) and 2(*n*+1). The spectrum of the output periodic intensity can be obtained by the Fourier transformation of Eq. (2), which is given by:

$$F(I_{out}) = I_b\delta(\omega_f) + \frac{I_{in}}{2}\begin{Bmatrix} \delta(\omega_f) + A_{2(n-1)}\{\delta[\omega_f - 2(n-1)] + \delta[\omega_f + 2(n-1)]\} \\ -iB_{2(n-1)}\{\delta[\omega_f - 2(n-1)] - \delta[\omega_f + 2(n-1)]\} \\ +A_{2(n+1)}\{\delta[\omega_f - 2(n+1)] + \delta[\omega_f + 2(n+1)]\} \\ -iB_{2(n+1)}\{\delta[\omega_f - 2(n+1)] - \delta[\omega_f + 2(n+1)]\} \end{Bmatrix} \tag{3}$$

where

$$A_{2(n-1)} = \frac{1}{2}\cos^2\Delta\cos 2\gamma \tag{4}$$

$$B_{2(n-1)} = \frac{1}{2}\cos^2\Delta\sin 2\gamma \tag{5}$$

$$A_{2(n+1)} = \frac{1}{2}\sin^2\Delta\cos(4\theta + 2\gamma) \tag{6}$$

$$B_{2(n+1)} = \frac{1}{2}\sin^2\Delta\sin(4\theta + 2\gamma) \tag{7}$$

Accordingly, with reference to equations (4)-(7), the three characteristic parameters are given through the magnitudes of the spectrum at the angular frequencies of 2(*n*-1) and 2(*n*+1):

$$\gamma = \frac{1}{2}\arctan[B_{2(n-1)} / A_{2(n-1)}] \tag{8}$$

$$\theta = \frac{1}{4}\arctan[B_{2(n+1)} / A_{2(n+1)}] - \gamma/2 \tag{9}$$

$$2\Delta = 2\arctan\{[A_{2(n+1)}^2 + B_{2(n+1)}^2]/[A_{2(n-1)}^2 + B_{2(n-1)}^2]\}^{1/4} \tag{10}$$

where $\gamma \in [-\pi/2, \pi/2]$, $\theta \in [-\pi/2, \pi/2]$ and $2\Delta \in [0, \pi]$. The characteristic retardation, obtained from Eq. (10), is map of the periodic parameter. If fringe orders above 0.5 are present, phase unwrapping algorithms have to be used to convert the data into a continuous map. It is noted from equations (4)-(7) that the characteristic angle is undefined when the characteristic retardation $\Delta=(m+1/2)\pi$ (m=0, 1, 2…) and the primary characteristic direction is undefined when the characteristic retardation $\Delta=m\pi/2$ (m=0, 1, 2…).The procedure of the phase-unwrapping and identifying the undefined regions is the same as described by Tomlinson [6].

It can also be noted that the angular rotation ratio can be operated at any value. To satisfy the requirements of efficiency and proper data accuracy, the angular rotation ratio should be optimized. In previous research, the angular rotation ratio is set as 3:1 [7]. In the process of image acquisition the polarizer is stepwise rotated over 360 degrees and the analyzer is rotated over 1080 degrees. To satisfy the requirement of the discrete Fourier analysis, the minimum number of the intensity images to be collected during one full rotation of the polarizer is nine. Obviously it is not efficient compared to the phase-stepping method. As seen from Eq. (3), the absolute values of $2(n-1)$ and $2(n+1)$ should be the integers to satisfy the requirements of proper data accuracy and as small as possible to improve the data collection efficiency. Accordingly the angular rotation ratio of 1:2 is the optimized value. In this way, the polarizer is still stepwise rotated over 360 degrees but the analyzer is only rotated over 180 degrees. The minimum number of the intensity images to be collected is now only five images. In the automated experimental apparatus, the rotary stages are used to position the polarizer and the analyzer. The duration of the measurement procedure is determined mainly by the maximum overall revolution of either the polarizer or the analyzer, which ever is the longer, over the speed of the rotary stages. The Fourier method operated at the angular rotation ratio of 1:2 therefore affords a considerable time saving over that at the angular rotation ratio of 3:1.

3. Experiments to test the proposed Fourier Method

3.1 Disc in Compression

To ascertain the efficiency and accuracy of Fourier method described above, the algorithms were first tested by a simulated experiment using Matlab. A photoelastic disc in diametral compression was generated and five Fourier-polarimetry images of the model are generated using Eq. (2) with the angular rotation ratio of 1:2. Fast Fourier transformation was used to process these images and then three characteristic parameters were determined by the magnitudes of the spectrum at the first and third angular frequency through Eq. (8) to (10). Figure 2 shows a comparison between the theoretical and simulated results of three characteristic parameters along the line between the two loading points. The simulated results were obtained also at the angular rotation ratio 3:1 using the Fourier method. Figure 2a shows the unwrapped continuous characteristic retardation. It can be seen that the results match each other very well. The characteristic angles presented in Figure 2c are all zeros except some undefined points, which is as expected for a two-dimensional model.

3.2 Three-dimensional Simulation

A three-dimensional birefringent model was simulated as described by Tomlinson [6]. The cylinder consisted of three photoelastic discs in diametral compression, which were arranged to align so that the loading points were at angle of 0^0, 22.5^0 and -45^0 to the horizontal reference axis. A three-dimensional stress field was created when viewed from the top/bottom of the cylinder. The same procedure as before was used to generate the Fourier-polarimetry images and then the three periodic characteristic parameters were determined using the Fourier method at the angular rotation ratios of 1:2 and 3:1 that are shown in Figure 3. These data clearly show that there is no difference in quality between the two rotation ratios.

3.3 Experimental Results

The following experimental procedure was implemented to verify the proposed Fourier method. A stress-frozen disc was placed in a plane polariscope. The analyser and polarizer were rotated simultaneously at the fixed ratios of 1:2 and 3:1 with respect to each other over one 360 revolution of the polarizer. The collection of 18 images for n=1:2 and n=3:1 were recorded at discrete intervals by a CCD camera connected to a PC. These images were then processed using the same algorithms described above to find the three characteristic parameters.

Figure 4 shows experimental data obtained at the rotation ratios of 1:2 and 3:1 respectively. It is shown that the three characteristic parameters have a similar distribution at the angular rotation ratios of 1:2 and 3:1. Figure 5 shows a comparison of the characteristic retardation measured by the angular rotation ratios 1:2 and 3:1 along the line shown in Figure 4. It is shown that they provide similar fringe orders and comparable accuracy in terms of inherent noise. Considering the efficiency of the data collection and the accuracy of the data analysis, the rotated ratio of 1:2 is the optimized choice for the Fourier method. It is noted that there are some undefined regions in the primary characteristic direction and the characteristic angle. These appear when the characteristic retardation $\Delta = m\pi/2$ (m=0, 1, 2…) for the primary characteristic direction, and when the characteristic retardation $\Delta = m\pi$ for the characteristic angle. This is a known phenomenon discussed by Tomlinson [6].

4. Sensitivity to noise

As seen from Figure 5, there are still some errors in experimental results. The magnitudes of the spectrum at the angular frequencies of $2(n\text{-}1)$ and $2(n+1)$ are affected not only by three characteristic parameters but also by the light intensity I_{in}. It is assumed that the light intensity is constant in the process of image acquisition when Eq. (3) is derived from Eq. (2). However, there are some noises introduced by an unstable light source and a non-uniform polarizer in a real experiment, which will result in inconstant light intensity. The sensitivity to noise measured by the angular rotation ratios 1:2 and 3:1 has been investigated and the resulting error in the three characteristic parameters is shown in Figure 6. Thirty six intensity images described by Eq. (2) were numerically generated from known prescribed three characteristic parameters with three different levels of noise (3dB, 10dB and 20dB). The Fourier transformation was then applied to obtain the measured three characteristic parameters. For Figure 6(a), the characteristic retardation was simulated from 0 to 0.5 fringe orders with the primary characteristic direction and the characteristic angle both fixed at 5º. For Figure 6(b), the primary characteristic direction is simulated from -40º to +40º with the characteristic retardation equal to 0.25 fringes and the characteristic angle equal to 5º. For Figure 6(c), the characteristic angle was simulated from -70º to +70º with the characteristic retardation equal to 0.25 fringes and the primary characteristic direction equal to 5º. It can be seen that the performance of the sensitivity to noise using the angular rotation ratios 1:2 and 3:1 are very similar for the three characteristic parameters. Figure 6(a) shows that the characteristic retardation has better performance against the noise when the fringe order is not close to $m\pi/2$ (m=0, 1, 2…) even when the SNR of the light intensity is 3dB. The SNR of the primary characteristic direction, which is shown in Figure 6(b), has better performance when the primary characteristic direction is close to zero degrees; however, it is heavily affected in the area close to $\pm\pi/4$ even when the SNR is 10dB. Accuracy of the characteristic angle shown in Figure 6(c) is independent of its magnitude but dependant on SNR. Overall the accuracy of Fourier method is therefore affected by the stability of the light source and the quality of the polarizer. The use of a fast Fourier transform means that many images can be sampled which would reduce the effect of noise and should increase the accuracy of the method. Using the same simulation method as was used in Figure 6, the noise was fixed at 10dB and different numbers of images (9, 36 and 144) were taken for the Fourier transformation and the measured characteristic parameters are shown in Figure 7. It is clear that the increase of the sampled images will result in the improvement of the accuracy. These simulated results also show comparable accuracy between the two rotation ratios.

5. Discussion and Conclusion

In this paper we have examined the Fourier method and determined an optimized rotation ratio. From our analysis the Fourier method using the optimized rotation ratio of 1:2 affords a considerable time saving over using the rotation ratio of 3:1 suggested by previous researchers, especially in the application of the tomographic photoelasticity for 3D stress measurement. The requirement of at least 36 scanning (5 degrees interval) data from six views of the object in the tomographic photoelasticity means that Fourier polarimetry has to be used 216 times [3]. For the angular rotation ratio 3:1, a full measurement cycle is expected to take over 12 hours excluding the time taken for manual re-positioning about horizontal axes. It is only about 4.5 hours using the angular rotation ratios 1:2, which means the experiment could be finished in a day. The apparatus is primarily automated and so operator input is negligible [9]. The simulated and experimental results also show the Fourier method using the rotation ratio of 1:2 can provide the comparable accuracy with that of 3:1. However in Figure 7 it is shown that up to 144 images could be required for each view in order to reduce noise even further, which may be required for the tomographic reconstruction method proposed in [3]. Therefore using the optimised rotation ratio becomes essential for efficient collection of data for tomographic reconstruction.

Figure 5 shows, as in phase stepping [6], that undefined zones appear due to an interaction between the characteristic parameters, but these can be easily identified and extrapolated over. Figures 6 demonstrates that noise in the system has a greater effect on the retardation measurements when $\Delta=m/2$ (m=0, 1, 2…), and the primary characteristic direction when close to $\pm\pi/4$, and so it is essential that the SNR is optimised by careful selection of quality experimental apparatus. It is considered that this effect may be eliminated by the extrapolation process over the undefined zones.

The apparatus which has been constructed for our experiments [9] currently has an SNR between 3 and 10 dB and it is believed that the stability of the light source and the quality of the polarizers contributes to this level. Further improvements may be expected by sampling an over-determined data set.

To conclude, an improvement has been made to the Fourier polarimetry method used to determine the three characteristic parameters used in integrated photoelasticity. Optimising the rotation ratio of polarizer to analyzer is essential for the efficient recording of large data sets required in tomographic photoelasticity and it has been shown that the optimised ratio gives results of equivalent accuracy as those used previously. It has been demonstrated however, that the method is sensitive to noise and careful selection of experimental apparatus is essential for applications in tomographic reconstruction.

References

1. H. Hammer and W. R. B. Lionheart, “Reconstruction of spatially inhomogeneous dielectric tensors via optical tomography,” J. OSA (A), 22 (2), 250-255 (2005)

2. H. Hammer, “Characteristic parameters in integrated photoelasticity: an application of Poincare’s equivalence theorem,” J. Modern Optics, 51, 597-618 (2004)

3. D. Szotten, R. A. Tomlinson, and W R B Lionheart, “Tomographic Reconstruction of Stress from Photoelastic Measurements using Elastic Regularization,” submitted to Inverse Problems, (2006)

4. S. Berezhna, I. Berezhnyy and M. Takashi, “Integrated photoelasticity through imaging Fourier polarimetry of an elliptic retarder,” Applied Optics, 40(5), 644-651 (2001)

5. Gibson, S, Tomlinson R A, Patterson, E A, (2003, June) Towards accurate full-field collection of characteristic parameters, Proceedings of the SEM Conference on Experimental and Applied Mechanics, Charlotte, North Carolina, USA, Paper No. 25

6. R. A. Tomlinson and E. A. Patterson, “The use of phase stepping for the measurement of characteristic parameters in integrated photoelasticity,” Experimental Mechanics, 42, (1), 43-50 (2002)

7. S. Berezhna, I. Berezhnyy and M. Takashi, “High resolution birefringence imaging in three-dimensional stressed models by Fourier polarimetry,” Applied Optics, 40(28), 4940-4946 (2001)

8. H. Aben, *Integrated Photoelasticity,* New York: McGraw-Hill, 1979.

9. Tomlinson, R A, Yang H, Szotten, D, and Lionheart, W R B, (June 2006), The Design and Commissioning of a Novel Tomographic Polariscope, Proceedings of the SEM Annual Conference on Experimental and Applied Mechanics, St Louis, USA, Paper No. 244

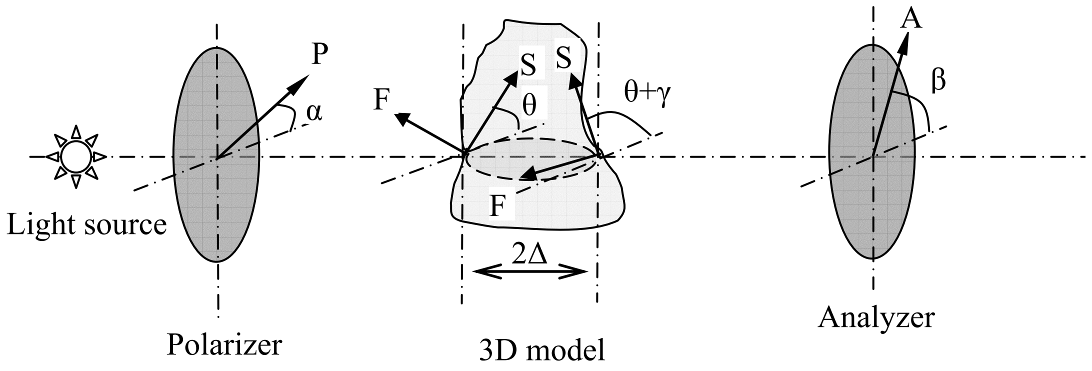

Figure 1 Configuration of a plane polariscope

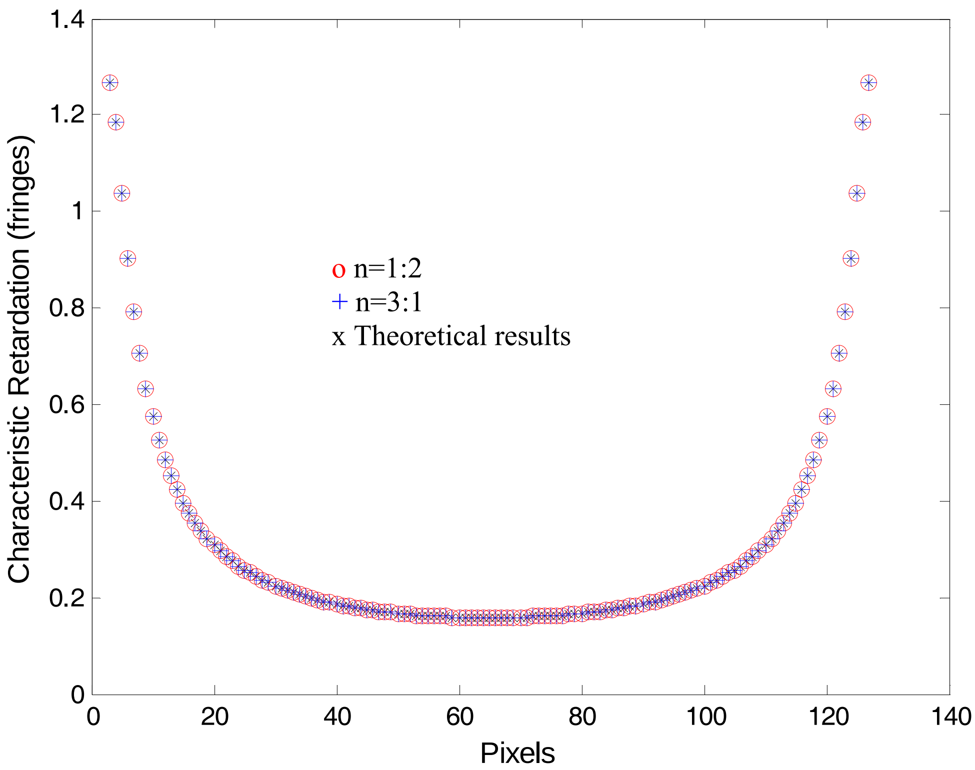

(a)

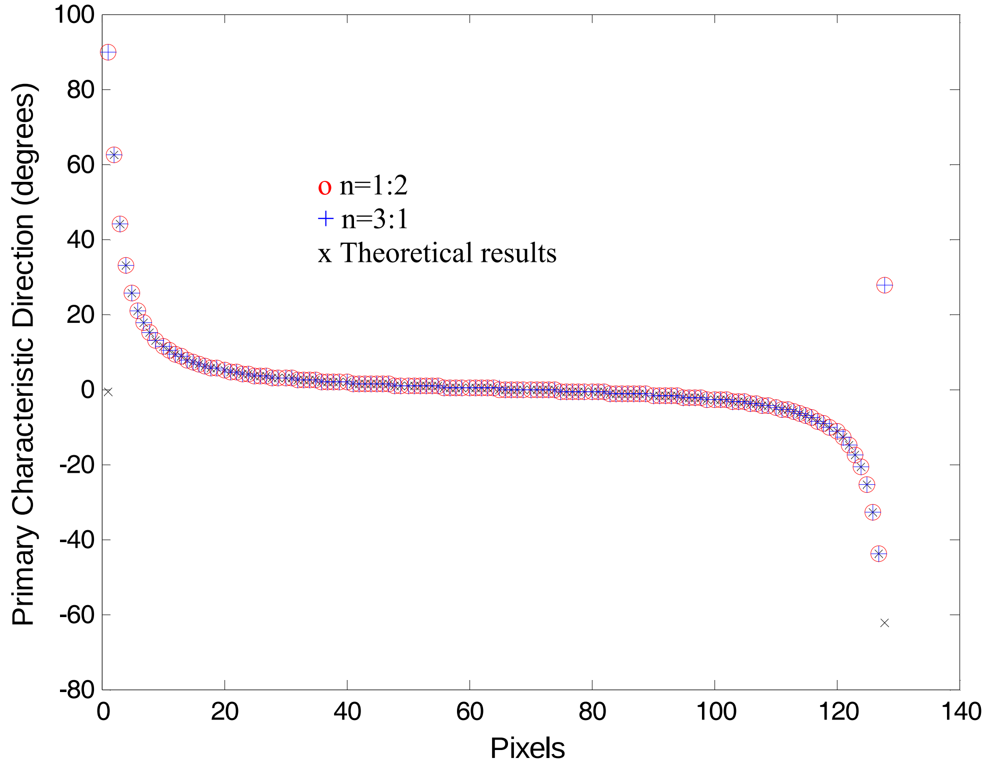

(b)

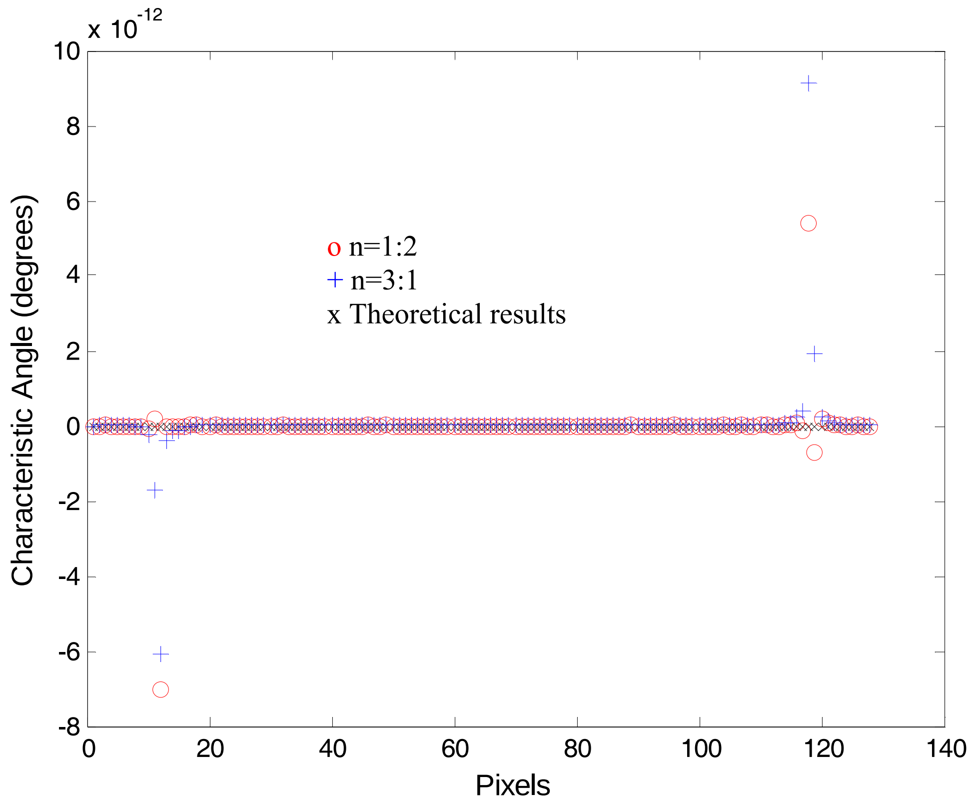

(c)

Figure 2 Simulated and theoretical results of the three characteristic parameters
(a) Characteristic retardation; (b) Primary characteristic direction; (c) Characteristic angle

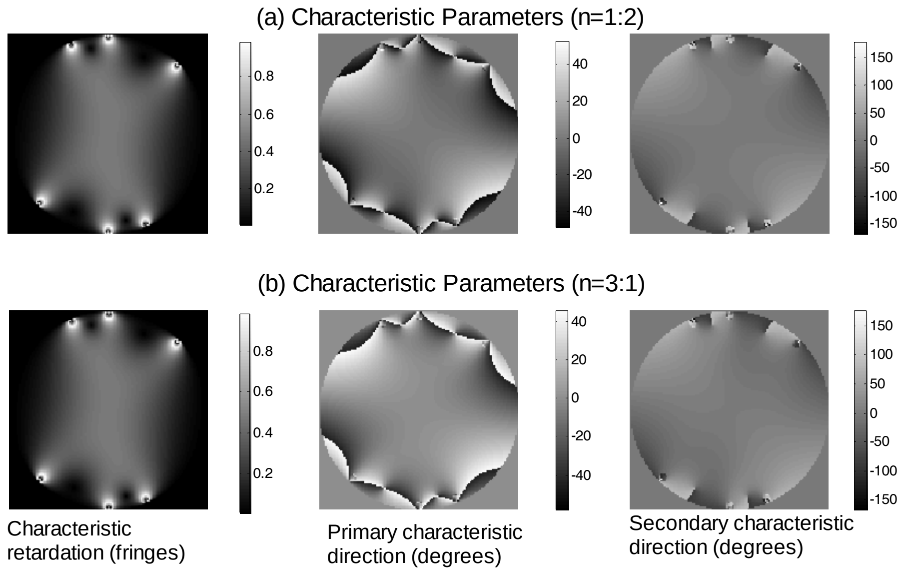

Figure 3 Three-dimensional simulation of a composite cylinder showing the periodic characteristic parameters for the angular rotation ratios (a) n=1:2 and (b) n=3:1

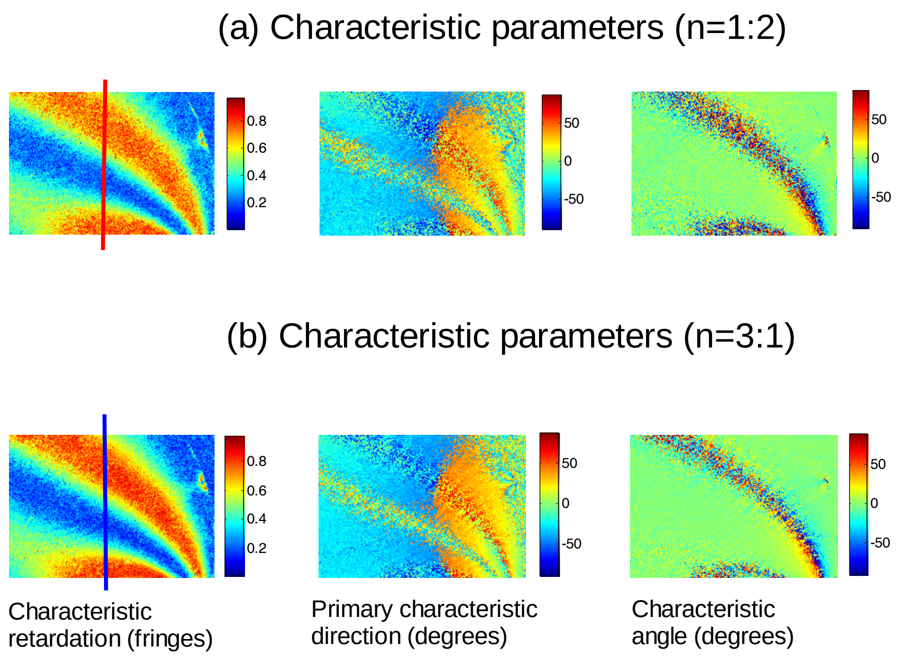

Figure 4 Experimental results the three characteristic parameters in a stress-frozen disc for the angular rotation ratios (a) n=1:2 and (b) n=3:1

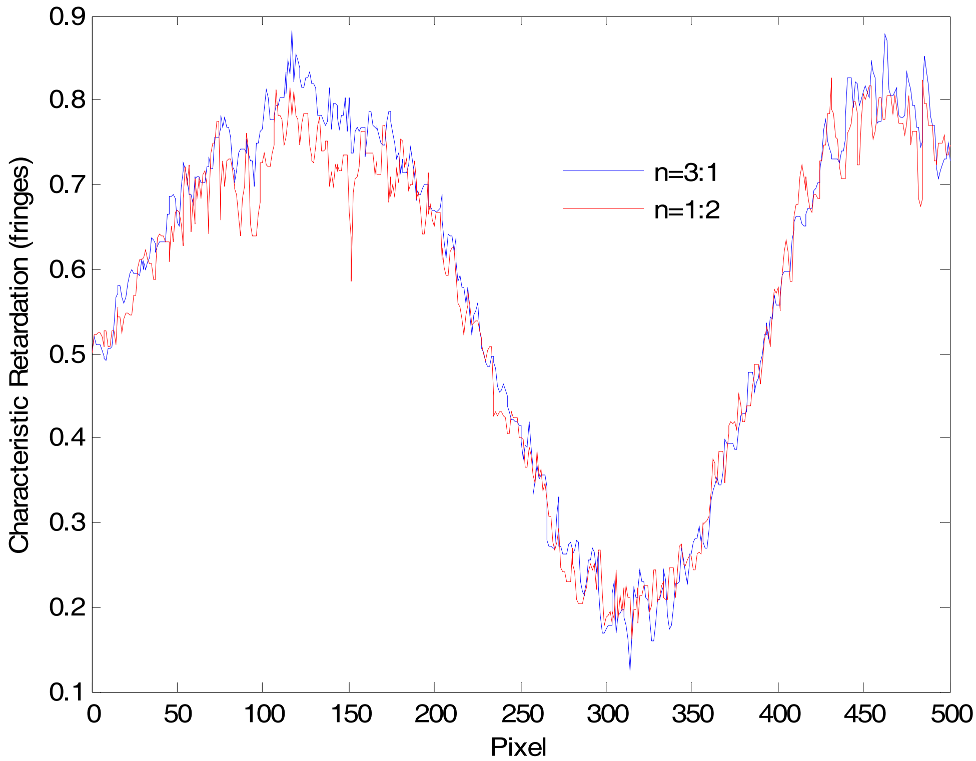

Figure 5 A comparison of the characteristic retardation measured by the angular rotation ratios 1:2 and 3:1 along the line shown in Figure 4

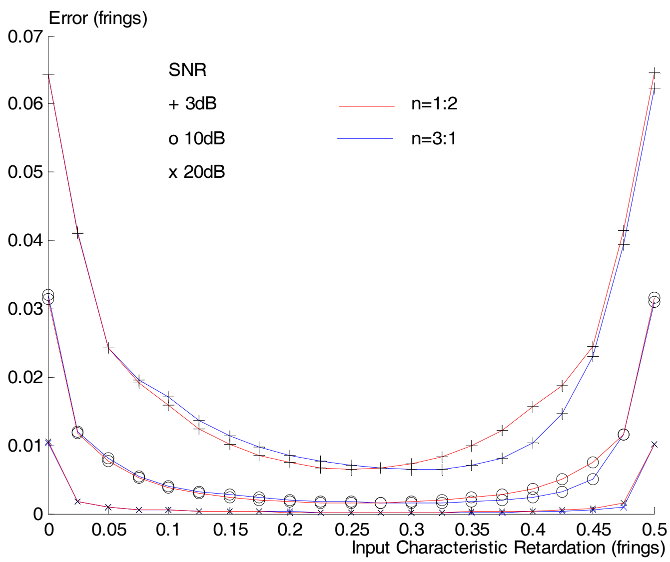

(a)

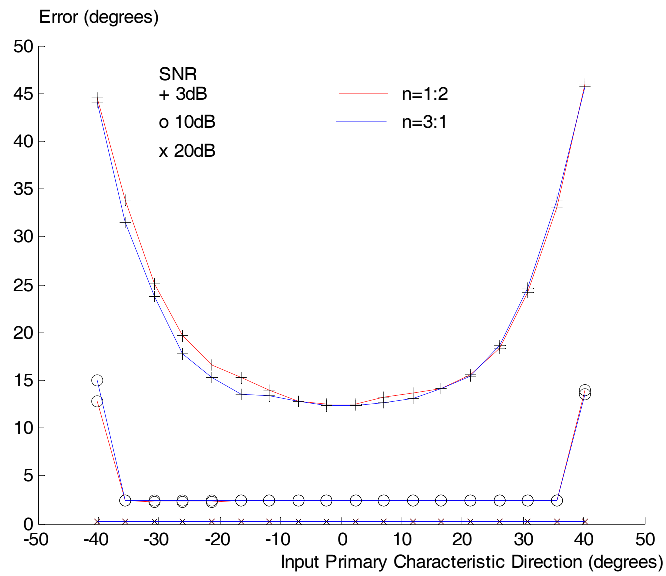

(b)

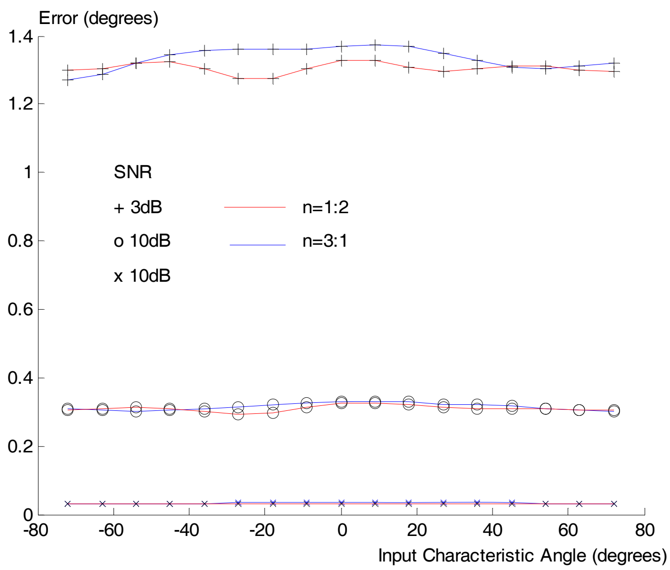

(c)

Figure 6 Simulated results of the sensitivity to noise of (a) characteristic retardation, (b) primary characteristic direction, and (c) characteristic angle

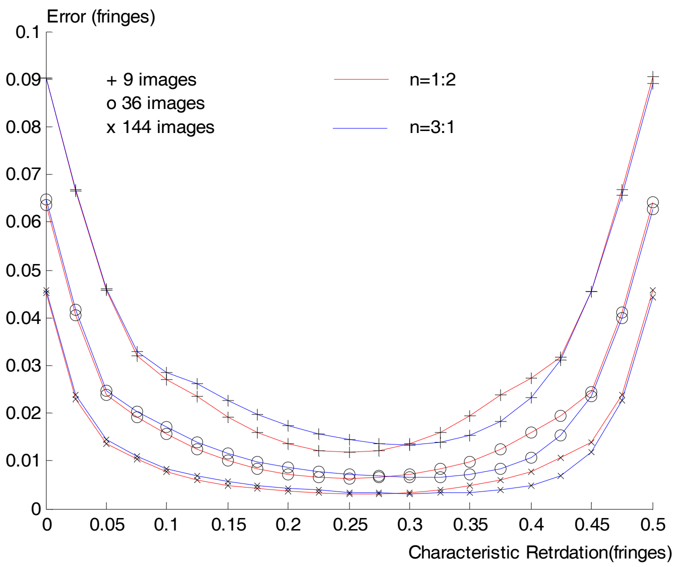

Error (fringes)
+ 9 images
o 36 images
x 144 images
n=1:2
n=3:1
0.1
0.09
0.08
0.07
0.06
0.05
0.04
0.03
0.02
0.01
0
0 0.05 0.1 0.15 0.2 0.25 0.3 0.35 0.4 0.45 0.5
Characteristic Retrdation(fringes)

(a)

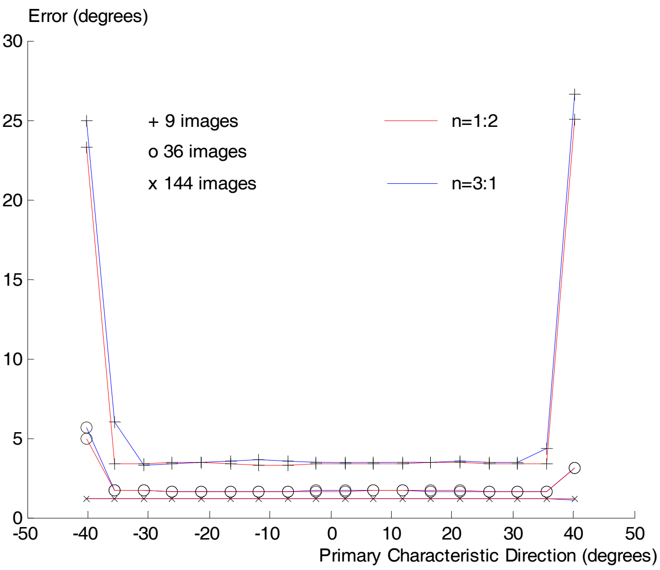

Error (degrees)
+ 9 images
o 36 images
x 144 images
n=1:2
n=3:1
30
25
20
15
10
5
0
-50 -40 -30 -20 -10 0 10 20 30 40 50
Primary Characteristic Direction (degrees)

(b)

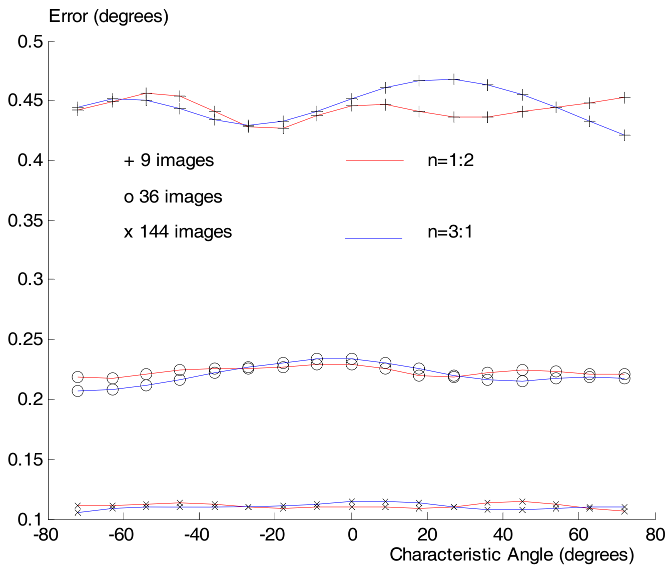

(c)

Figure 7 The effect of different numbers of sampling images on (a) characteristic retardation, (b) primary characteristic direction, and (c) characteristic angle